

On the correlation between solid-particle erosion and fracture parameters in SiC*

J. L. ROUSBORT †, HJ. MATZKE

Commission of the European Communities, Joint Research Centre, Karlsruhe Establishment, European Institute for Transuranium Elements, Postfach 2266, D-7500 Karlsruhe, Federal Republic of Germany

The fracture toughness, K_{Ic} , for a hot-pressed SiC and three types of reaction-bonded SiC has been measured using the Hertzian indentation technique with spherical indentors whose radii varied from 2.5 to 10 mm. Excellent agreement between the toughness measured by this technique and the published K_{Ic} value measured using double torsion is obtained for the hot-pressed SiC. The Vickers hardness, H , which was also measured, and K_{Ic} have been used to predict the solid-particle erosion rate, ΔW , given by $\Delta W \propto H^a K_c^b$ where the values of the exponents a and b depend on the details of the erosion model. The predicted rates are not in agreement with the measured rates. This discrepancy is probably due to the fact that the models are insensitive to microstructure.

1. Introduction

Solid-particle erosion is a very serious problem which can cause premature failure of components used in many high technology energy conversion processes, i.e. coal gasification. Impingement of moving, angular particles onto the surface of a brittle solid causes the formation of lateral cracks which intersect the surface, causing material removal and seriously degrading strength. An understanding of the basic erosion mechanisms and how they depend on fundamental materials properties is necessary to develop erosion-resistant materials.

Two previous studies of the solid-particle erosion [1, 2] of brittle materials have shown that while many predictions of both the quasi-static [3] and the elastic-impact [4] model are followed, the models are not entirely successful in describing the materials parameters of the erosion rate. The length of the lateral cracks, c , is proportional to $(P_{max}/K_c)^{2/3}$ where P_{max} is the maximum contact force and K_c ‡ the fracture toughness. The material removal is proportional

to c^2 times the depth of penetration of the impacting particle. The quasi-static model of Wiederhorn and Lawn [3] calculated the force and penetration depth based on the conversion of the kinetic energy of the impacting particle modelled as a sharp indenter into the plastic work of the target. The Evans *et al.* [4] model assumes that the contact pressure is equal to the dynamic pressure set up when a spherical particle impacts the target surface. The depth of penetration and the mean interface velocity are calculated from a one-dimensional analogue.

Both models predict that the form of the steady-state erosion rate (in units of grams of material removed per gram of impacting material) is given by

$$\Delta W \propto D^m v^n \rho^q H^a K_c^b \quad (1)$$

where the particle properties are given by its diameter D , velocity v , and density ρ ; the hardness H , and fracture toughness K_c are the important target properties. The predicted velocity exponent, n , varies between 2.4 and 3.2 depending on the model. In reality, the experimental values depend

*Part of this work was supported by the US Department of Energy.

†Permanent address: Materials Science Division, Argonne National Laboratory, Argonne, Illinois 60439, USA.

‡ The subtle differences between the fracture toughness measured in this study, K_{Ic} , and the fracture toughness used to characterize the lateral cracks responsible for erosion, K_c , will be ignored.

on the size of the projectiles which probably change the contact conditions [5]. The size exponent, m , is close to the value of $2/3$ predicted by both models if threshold effects are taken into consideration [6]. The density exponent, q , is also model-dependent [3, 4]. It is the objective of this paper to explore the dependence of ΔW on the materials parameters. The exponents given by the quasi-static model are $a = 0.11$ and $b = -1.3$ and by the dynamic model $a = -0.25$ and $b = -1.3$ again. Recently, Wiederhorn and Hockey [2] have used dimensional analysis and an empirical fit to data obtained on a range of brittle solids to calculate that $a = 0.48$ and $b = -1.9$.

The two previous studies which examined the dependence of ΔW on H and K_{Ic} concentrated on a wide variety of materials ranging from glass to MgO [1, 2]. Further, the authors generally used literature values of H and K_{Ic} . The present study has concentrated on three types of reaction-bonded (RB) SiC, where the erosion rate has been accurately measured over a wide range of velocities and particle sizes [7, 8] and for at least two angles of incidence. These samples have different microstructures, primarily in the amount and distribution of free silicon. Furthermore, the hardness and the fracture toughness of the samples used in the erosion studies were measured, therefore providing a sound basis for comparison.

The Hertzian indentation technique [9] was used to measure the fracture toughness. In this technique, a spherical indenter of radius, R , is pressed into the flat surface of a SiC sample with a load, P , and the critical load, P_c , for the formation of a Hertzian ring crack of radius, r , is measured. The formation of the cracks and their sizes are measured optically. The surface fracture energy, γ_F which is related to K_{Ic} by

$$2\gamma_F = [(1 - \nu^2)/E] K_{Ic}^2$$

where ν is Poisson's ratio and E is Young's modulus, can be calculated using the numerical integration of the crack extension function published by Warren [9] which gives the critical load P_c as

$$P_c = \frac{\beta k R \gamma_F}{(1 - \nu^2)} \frac{a}{c''} [\phi(c'')]^{-2} \quad (2)$$

where $[\phi(c'')]^{-2}$ is the integral over the crack path of the variable principal tensile stress normal to the crack path, c'' the crack depth, β a constant, $k = \frac{9}{16} [(1 - \nu^2) + (1 - \nu'^2)E/E']$ where the primed

values refer to the indenter, a is the contact radius calculated from $a^3 = 4kPR/3E$. This technique has been successfully applied to small samples of materials such as UO_2 [10], ThO_2 [11, 12], (U, Pu)C [13], and transition metal carbides [9].

The value of the constant β calculated assuming that the cone crack has the same stress intensity factor as a plane internal crack is $8\pi^3/27$. This is clearly an approximation and it is therefore very desirable to calibrate the Hertzian technique. That is to measure K_{Ic} using the indentation technique in a material where K_{Ic} had been measured using a more conventional technique. Therefore the indentation technique was used to measure K_{Ic} on a hot-pressed (HP) SiC whose erosion rate was also known [14] and whose fracture toughness had been measured in double torsion by Wiederhorn and Tighe as quoted in [15]. This is the first time that the two techniques have been directly compared. A previous comparison on WC involved extrapolated values [16].

2. Experimental procedure

The materials used in this study are listed in Table I, along with their manufacturer, fabrication method, density, Vickers hardness, volume per cent of free silicon, Young's modulus, and Poisson's ratio. The microstructure of HP-NC203 [14] consists predominantly of a single phase of 95 to 99% pure SiC having an average grain size of 2 to $3 \mu m$ and a maximum grain size of $\sim 10 \mu m$. The RB-SiC NC430 is a two-phase duplex-microstructure ceramic composed of high-purity SiC. The microstructure [7] consists of large SiC grains occupying a volume fraction of ~ 0.5 while the matrix surrounding them is a two-phase mixture of small SiC grains and free silicon containing a volume fraction of ~ 0.35 SiC and ~ 0.15 silicon. The RB-SC-1 and RB-SC-2, whose microstructures are shown in Fig. 1, contain randomly distributed agglomerates of unequal size of free silicon. SC-1 contains at least 0.20 volume fraction of free silicon while SC-2 has at least 0.13 volume fraction of silicon. These are the lower limits since it was not possible to measure very small silicon agglomerates.

Both the Hertzian indentation technique [9-11] and the measurements of the steady-state erosion rate [7, 8, 14] have been described in detail. It is sufficient here to note that K_{Ic} and H measurements were made on the rear-side of

TABLE I Properties of SiC investigated

Material designation	Fabrication method	Free silicon (%)	Density* ($\times 10^3 \text{ kg m}^{-3}$)	VHN [†] (GPa)	E^{\ddagger} (GPa)	ν^*	$\Delta W \times 10^3$ (g g^{-1})
Norton NC203	Hot-pressed	—	3.26	29.7 ± 1	441	0.168	2.0 [14]
Norton NC430	Reaction-bonded	10.6*	3.1	27.7 ± 2	383	0.24	12.2 [1]
Coors SC-1	Reaction-bonded	20	3.03	25.7 ± 3	403	0.19	10.0 [8]
Coors SC-2	Reaction-bonded	13	3.1	24.3 ± 1.6	404	0.19	4.5 [8]

*Data supplied by manufacturer.

[†]Load-independent Vickers hardness measured in the range of 100 to 400 g.

[‡]Data supplied by manufacturer, but verified using the time-of-flight method.

samples previously used in the erosion studies which were polished to $1 \mu\text{m}$ diamond paste.

3. Results

A typical steady-state erosion rate, ΔW is given in Table I. In this case the data was obtained using angular Al_2O_3 particles of $270 \mu\text{m}$ diameter impinging the target at normal incidence at a velocity of 108 m sec^{-1} . The ΔW of HP-NC203 is included for reference only since it is known to be anomalous [14].

The ΔW values for NC430 and for SC-1 are approximately equal and at least twice as large as ΔW measured for SC-2. These relative rates remain approximately constant for velocities between 50 and 150 m sec^{-1} , for incident angles of 45° and 90° , and for particle sizes from 37 to $270 \mu\text{m}$. For smaller particle sizes all RB-SiC

samples exhibit a pronounced change from the predicted slope in the ΔW against D data, probably reflecting threshold effects [7].

A typical probability curve for formation of Hertzian cracks with four sizes of steel indentors ($\nu' = 0.29$ and $E' = 210 \text{ GPa}$) as a function of P is shown in Fig. 2. The probability to failure represents the percentage of formation of a ring crack in at least five attempts at a given load. The cracks were easily observable under an optical microscope and were usually accompanied by acoustic emission activity. They were very circular and their path was independent of the free silicon. The critical load, P_c , which is operationally defined as the load at which the failure probability = 0.5 , is shown as a function of indenter radius in Fig. 3. The error bars indicate the uncertainty in defining P_c from the data of Fig. 2. Finally,

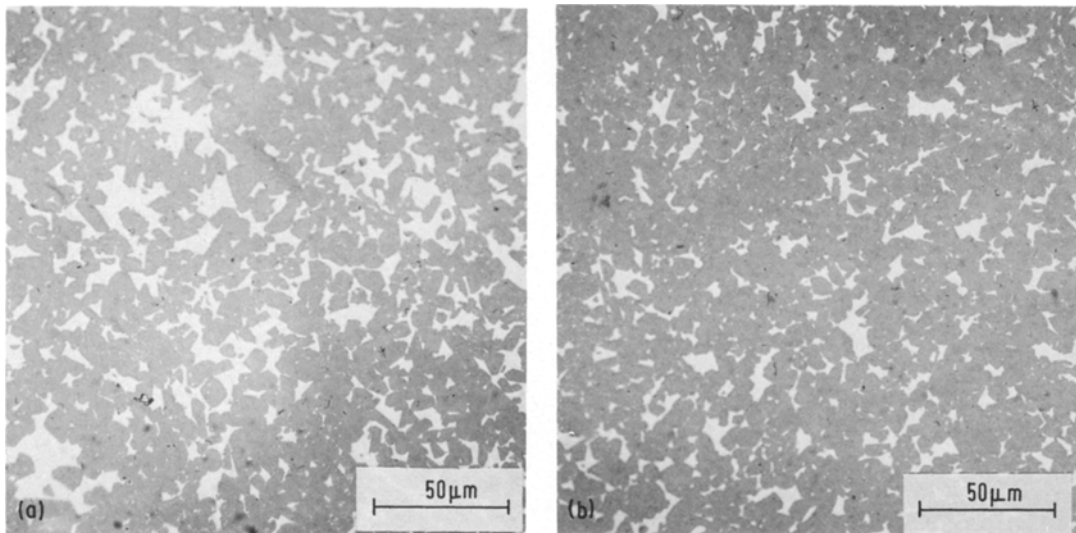


Figure 1 (a) Microstructure of SC-1, and (b) microstructure of SC-2.

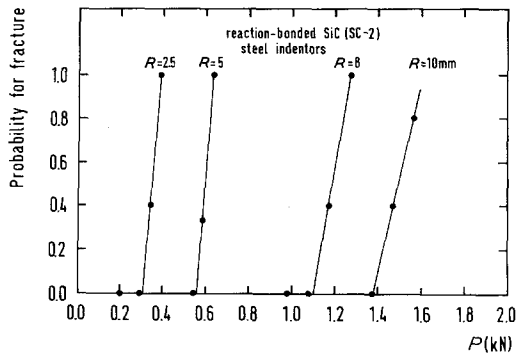


Figure 2 The probability of formation of a Hertzian ring crack shown as a function of applied load for steel indentors of 2.5, 5, 8, and 10 mm radius for SC-2.

the results for all of the SiC samples are shown in Fig. 4, where data points are omitted for clarity.

In all cases Auerbach's law, which predicts a linear relationship between P_c and R intersecting the origin, is obeyed. Therefore, the results may be analysed according to Equation 2 to evaluate γ_F and K_{Ic} . These values are summarized in Table II along with those of $(a/c'')[\phi'']^{-2}$ which were obtained using Warren's results [9] with the measured value of γ , the calculated value of a , and E and ν as given in Table I. It should be mentioned that some data was obtained using Si_3N_4 spheres in order to reduce the elastic mismatch between the SiC sample and the steel sphere. As expected, the slopes of the P_c against R curves were lower reflecting the lower k , but the values for γ_F and K_{Ic} using either material as an indenter agreed to within experimental error.

The errors in K_{Ic} are expected to be no more than $\pm 10\%$. The slopes in the P_c against R curves are accurate to $\pm 10\%$ which results in an error of $\pm 5\%$ in K_{Ic} . The crack extension function for

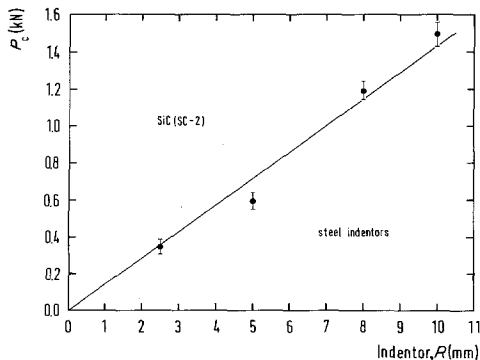


Figure 3 The critical load to form a ring crack shown as a function of indenter radius for SC-2.

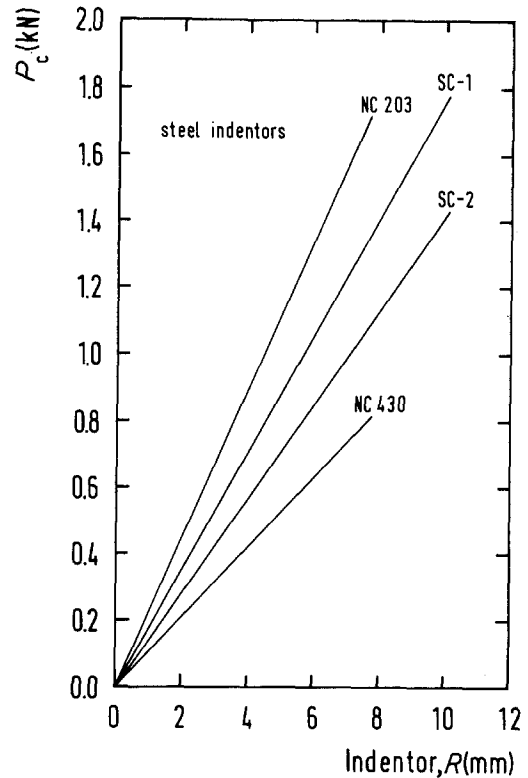


Figure 4 The critical load as a function of indenter radius for the four SiC samples investigated.

$r/a > 1.05$ is relatively insensitive to changes in ν for the range of ν (0.17 to 0.24) encountered in this work. For example, an error of $\pm 10\%$ in ν would result in $\pm 4\%$ uncertainty in K_{Ic} . Small uncertainties arise because of uncertainties in E and E' and errors in the measurement of r . The scatter in the determination of P_c was large in the case of 7.5 mm radius indentors in HP-NC203. This may be due to flaw statistics because large indentors require larger flaw sizes. Warren's [9] analysis may be used to estimate that the threshold flaw size in this case should be $\sim 15 \mu\text{m}$, considerably larger than the grain size. Grain boundary weakness is responsible for enhanced erosion [14]. In the case of the RB-SiC samples the flaws necessary to nucleate the ring cracks

TABLE II Average values of fracture parameters obtained using steel indentors of various radii

Material	r/a	$\frac{a}{c''} [\phi'']^{-2}$	γ_F (J m^{-2})	K_{Ic} ($\text{MN m}^{-3/2}$)
NC203	1.09	900	16.2	3.8
NC430	1.12	1700	4.3	1.9
SC-1	1.09	1100	11.0	3.0
SC-2	1.14	1100	9.6	2.8

may simply be the Si–SiC interface. Of course, the flaws could possibly be surface scratches produced by polishing. In this case, however, all measurements would be limited by flaw statistics. An examination of the probability against load curves shows that this does not appear to be the case.

4. Discussion

The fracture toughness of the HP-NC203 as measured by the Hertzian indentation technique using $\beta = 9.18$ is $K_{Ic} = 3.8 \text{ MN m}^{-3/2}$. The excellent agreement with the value of $4.0 \text{ MN m}^{-3/2}$ measured with the more conventional double torsion technique [15] is very satisfying. The agreement indicates, at least for this material, that the much less complicated indentation technique used in conjunction with Warren’s analysis with no adjustable parameters is reliable. Sharp indentors require a “calibration constant” which needs a prior knowledge of K_{Ic} measured conventionally [15]. The fact that the value of K_{Ic} determined conventionally agrees with the value of K_{Ic} determined by Hertzian indentation using $\beta = 9.18$ suggests that the cracks which form in HP-SiC closely approximate the plane crack modelled in the calculations. The HP-SiC is pure, fully dense, and homogeneous.

The attempt to correlate the measured K_{Ic} values given in Table II and the Vickers hardness values given in Table I with ΔW can be made using Equation 1 with the exponents from the various models. This correlation is presented in Table III where the first column refers to the static model [3], the second to the dynamic model [4] and the the third to the recent values of a and b derived by dimensional analysis [2]. These relations can be easily seen from Table IV which presents the predicted normalized erosion rate and the measured erosion rate. The rates are normalized with respect to the ΔW of SC-1. All models predict that the erosion rate of SC-1 and SC-2 should be approximately equal and approximately 1/2 that of NC430. The actual fraction depends on the model. However, as previously mentioned, the ΔW for SC-2 is approximately

TABLE III Values of $\Delta W \propto H^a K_{Ic}^b$ calculated for the various steady-state erosion models

Material	$H^{0.11} K_{Ic}^{-1.3}$ [3]	$H^{-0.25} K_{Ic}^{-1.3}$ [4]	$H^{0.48} K_{Ic}^{-1.9}$ [2]
NC203	0.54	0.013	11.1
NC430	1.34	0.034	40.0
SC-1	0.73	0.019	16.2
SC-2	0.80	0.021	18.0

Units of H are MN m^{-2} and units of K_{Ic} are $\text{MN m}^{-3/2}$.

1/2 that of the ΔW for SC-1 which is approximately equal to the ΔW for NC430. Therefore, the erosion rates cannot be rationalized solely on the basis of H and K_{Ic} .

On the other hand, the models would predict that ΔW for NC430 is ~ 2 times larger than ΔW for SC-2, close to the factor of ~ 3 observed. Similarly, the proposed correlations predict that ΔW for NC430 is ~ 3 times that of NC203. The observed factor is 6. It should be cautioned, however, that the ΔW of the HP-NC203 may still be affected by an additional contribution of erosion which arises because of the grain boundaries, even at the large particle size chosen to minimize both this contribution and threshold effects.

This investigation therefore agrees with the previous studies [1, 2] in concluding that no model of solid-particle erosion can completely describe the dependence of ΔW on the materials parameters H and K_{Ic} . It has been previously suggested that the discrepancies are due to microstructural effects [2, 14] or to the statistical way in which particles impact the surface. While the details of these processes were beyond the scope of this study, a few comments are in order.

Under the conditions of erosion used in Table I, pure silicon has a $\Delta W = 50 \times 10^{-3} \text{ g g}^{-1}$ [6], a much higher value than for the pure HP-SiC. This, in fact, leads to a “mesa” effect whereby with small particles the free silicon is preferentially eroded away leaving “mesas” of SiC behind [7]. On this basis alone one would expect the ΔW of SC-1 which has a larger volume fraction of free silicon to be larger than ΔW for SC-2, as observed, but not predicted. Furthermore, one might also

TABLE IV Predicted and measured erosion rates normalized with respect to ΔW for SC-1

Material	$(\Delta W/\Delta W_{SC-1})_{\text{predicted}}$	$(\Delta W/\Delta W_{SC-1})_{\text{measured}}$
NC430	1.8 to 2.5	1.2
SC-1	1	1
SC-2	1.1	0.45

expect that because the free silicon in SC-2 is more homogeneously distributed, resulting in smaller agglomerates than in the NC430, ΔW for SC-2 would be smaller than ΔW for NC430, as observed, but again not predicted. The argument outlined above seems able to explain the erosion results in a self-consistent fashion.

It is, however, harder to rationalize the K_{Ic} results except to note that it might be expected that K_c of the fine-grained HP-SiC would be larger than that of the RB-SiC, as observed. On the other hand, if the fracture toughness of the three RB-SiC are compared, it may be concluded that the volume fraction of free silicon seems to matter less than the distribution of free silicon since K_{Ic} (SC-1) $\approx K_{Ic}$ (SC-2) $\approx 1.5 K_{Ic}$ (NC430).

It is possible that in a two-phase ceramic, the fracture toughness which reflects an average bulk property is by itself insufficient to describe a local event such as erosion. Also the values of H reflect only the bulk SiC phase, the hardness of pure silicon being $\sim 30\%$ less than that of SiC. However, the factor of two difference between ΔW for SC-1 and SC-2 cannot be explained by a simple average of K_c and H over the volume fractions of the silicon and SiC phases. It is clear that not only are more experiments necessary, but that also the details of crack initiation and propagation have to be examined carefully before it may be possible to refine the erosion models.

5. Summary

1. The Hertzian indentation technique analysed according to Warren with no adjustable parameters and the double torsion technique yield the same value of fracture toughness for a hot-pressed SiC (NC203).

2. The hardness and fracture toughness of three types of reaction-bonded SiC have been measured and the values have been used to predict the solid-particle erosion rate. None of the existing models of erosion is entirely satisfactory indicating that

microstructural aspects must be incorporated into the erosion theory.

Acknowledgements

The authors were pleased to receive the erosion data of Dr A. P. L. Turner (ANL) on SC-1 and SC-2 prior to publication. They are also grateful to Mr M. Modery (TU) who performed the hardness measurements, Dr C. Sari (TU), who measured the volume fraction of free silicon and Dr C. Politis (KfK) who confirmed the Young's modulus.

References

1. M. E. GULDEN, *J. Amer. Ceram. Soc.* **64** (1981) C59.
2. S. M. WIEDERHORN and B. J. HOCKEY, *J. Mater. Sci.* **18** (1983) 766.
3. S. M. WIEDERHORN and B. R. LAWN, *J. Amer. Ceram. Soc.* **62** (1979) 66.
4. A. G. EVANS, M. E. GULDEN and M. ROSENBLATT, *Proc. Roy. Soc.* **361** (1978) 343.
5. R. O. SCATTERGOOD and J. L. ROUTBORT, *Wear* **67** (1981) 227.
6. J. L. ROUTBORT, R. O. SCATTERGOOD and E. W. KAY, *J. Amer. Ceram. Soc.* **63** (1980) 635.
7. J. L. ROUTBORT, R. O. SCATTERGOOD and A. P. L. TURNER, *Wear* **59** (1980) 363.
8. A. P. L. TURNER, unpublished data (1982).
9. R. WARREN, *Acta Met.* **26** (1978) 1759.
10. HJ. MATZKE, T. INOUE and R. WARREN, *J. Nucl. Mater.* **91** (1980) 205.
11. HJ. MATZKE, *J. Mater. Sci.* **15** (1980) 739.
12. T. INOUE and HJ. MATZKE, *J. Amer. Ceram. Soc.* **64** (1981) 355.
13. HJ. MATZKE, V. MEYRITZ and J. L. ROUTBORT, *ibid.* in press.
14. J. L. ROUTBORT and R. O. SCATTERGOOD, *ibid.* **63** (1980) 593.
15. G. P. ANSTIS, P. CHANTIKUL, B. R. LAWN and D. B. MARSHALL, *ibid.* **64** (1981) 533.
16. R. WARREN and HJ. MATZKE, International Conference on the Science of Hard Materials, Jackson Lake, August 1981, to be published.

Received 2 August

and accepted 12 November 1982